Field Testing LIDAR Based Feed-Forward Controls on the NREL Controls Advanced Research Turbine

Preprint

Andrew K. Scholbrock, Paul A. Fleming, Lee Jay Fingersh, and Alan D. Wright
National Renewable Energy Laboratory

David Schlipf and Florian Haizman
University of Stuttgart

Fred Belen
BlueScout Technologies

To be presented at the 51st AIAA Aerospace Sciences Meeting, including the New Horizons Forum and Aerospace Exposition
Grapevine, Texas
January 7-10, 2013

NREL is a national laboratory of the U.S. Department of Energy, Office of Energy Efficiency & Renewable Energy, operated by the Alliance for Sustainable Energy, LLC.

Conference Paper
NREL/CP-5000-57339
January 2013

Contract No. DE-AC36-08GO28308

Available electronically at http://www.osti.gov/bridge

Available for a processing fee to U.S. Department of Energy
and its contractors, in paper, from:

U.S. Department of Energy
Office of Scientific and Technical Information
P.O. Box 62
Oak Ridge, TN 37831-0062
phone: 865.576.8401
fax: 865.576.5728
email: mailto:reports@adonis.osti.gov

Available for sale to the public, in paper, from:

U.S. Department of Commerce
National Technical Information Service
5285 Port Royal Road
Springfield, VA 22161
phone: 800.553.6847
fax: 703.605.6900
email: orders@ntis.fedworld.gov
online ordering: http://www.ntis.gov/help/ordermethods.aspx

Cover Photos: (left to right) PIX 16416, PIX 17423, PIX 16560, PIX 17613, PIX 17436, PIX 17721

Printed on paper containing at least 50% wastepaper, including 10% post consumer waste.

Field Testing LIDAR-Based Feed-Forward Controls on the NREL Controls Advanced Research Turbine

Andrew Scholbrock
Paul Fleming
Lee Fingersh
Alan Wright
National Wind Technology Center
National Renewable Energy Laboratory
Golden, Colorado

David Schlipf
Florian Haizmann
University of Stuttgart

Fred Belen
BlueScout Technologies

Researchers at the National Renewable Energy Laboratory (NREL) and the University of Stuttgart are designing, implementing, and testing advanced feedback and feed-forward controls for multimegawatt wind turbines that will help reduce the cost of wind energy. Past wind turbine controllers have depended on turbine feedback measurements to determine the controller pitch commands. In this setup, wind speed disturbances can only be corrected after their effects have been detected in the turbine's loads and dynamic response, which causes a delayed control response due to turbine and pitch actuator dynamics. LIght Detection And Ranging (LIDAR) systems can provide information regarding the approaching wind field to the controller in advance, thereby increasing the controller's available reaction time and allowing pitch actuation to occur in advance to mitigate wind disturbance effects. Feed-forward control algorithms that use these "look ahead" wind speed measurements can improve load mitigation and controller performance compared to feedback only controllers. This paper describes the development and field testing of a feed-forward collective pitch control algorithm to show its effects on speed regulation in above-rated wind speeds. The controller is implemented and field tested on one of the Controls Advanced Research Turbines (CARTs) at NREL. The wind speed measurements to the feed-forward controller are provided by BlueScout Technologies' Optical Control System (OCS) LIDAR mounted on the nacelle of the CART3. Results show that inclusion of the LIDAR measurement into the control system leads to further rejection of the wind disturbance at low frequencies when compared to feedback alone. This in turn provides confidence that LIDAR technology could be used to obtain load reductions with wind turbine controls.

Introduction

Control can improve the performance and fatigue life of wind turbines by enhancing energy capture and reducing dynamic loads. Researchers at the National Renewable Energy Laboratory (NREL) and the University of Stuttgart have implemented and field tested advanced light detection and ranging (LIDAR)-based feed-forward controls on the Controls Advanced Research Turbines (CARTs), turbines specifically configured to test advanced control algorithms, at NREL. Typical commercial wind turbines operate with variable-speed and variable-pitch controls. In below-rated wind speeds (referred to as Region II) the generator torque is controlled to extract maximum power from the wind while blade pitch is held constant. In above-rated wind speeds (referred to as Region III) the generator torque is held constant, while blade pitch is used to regulate the rotational speed of the turbine using proportional-integral (PI) control.

Previous papers have shown that advanced feedback controllers can be designed to regulate turbine speed in Region III and to enhance damping of flexible turbine modes.[1–5] These controls depend on typical turbine feedback measurements, such as generator speed and tower-top acceleration. The effect of wind speed disturbances are accounted for by including a PI controller in the feedback loop and using turbine measurements to estimate this disturbance.[3]

New LIDAR systems can be attached to the turbine's nacelle and pointed upwind of the machine to provide information about the wind disturbance before it affects the turbine. Properly designed feed-forward controllers can take advantage of this "look-ahead" information, preparing the wind turbine in advance to better mitigate the effects of these disturbances,[6] rather than waiting for the effects to be detected in the feedback signals.

NREL and the University of Stuttgart, in collaboration with the LIDAR manufacturer BlueScout Technologies, developed and field tested feed-forward controllers on the NREL 3-bladed Controls Advanced Research Turbine (CART3) using BlueScout Technologies' optical control system (OCS) LIDAR as the feed-forward wind measurement sensor.

This paper describes the development and field testing of a feed-forward controller to be used to reject the wind disturbance in Region III wind conditions. The LIDAR-based feed-forward controller commands collective blade pitch that is added to a standard baseline feedback PI controller. This feed-forward controller is specialized to use LIDAR wind speed measurement data obtained from the OCS LIDAR.

Researchers compared the controller's speed regulation performance using the same feedback controller with and without the feed-forward update. The goal of this paper is to isolate the effect of including LIDAR feed-forward on the controller's speed regulation performance. Future controllers will be able to take advantage of these results by focusing on other control objectives (e.g. load reduction) without compromising tight speed regulation.

In this paper, we describe the specifications of the CART3 (Fig. 1) and the LIDAR system used for this study and provide an overview of feed-forward control design. We then present the field-test results and analyses that show improved disturbance rejection.

Figure 1: CART3 experimental wind turbine at the NWTC south of Boulder, Colorado. (NREL/PIX# 21664)

1. CART3 Description

Researchers at the National Wind Technology Center (NWTC) at NREL have used the 2 and 3-bladed Controls Advanced Research Turbines (CART2 and CART3) sited at the NWTC to test control systems for more than a decade. The NWTC is located east of the Front Range near Boulder, Colorado, USA, where wind conditions are well suited for advanced controls research. The CART3, converted from a 2-bladed turbine to a 3-bladed turbine to perform experiments for advanced controls research,[7, 8] was used for this study. Figure 1 shows the CART3 and Table 1 presents the turbine's basic specifications.

Table 1: CART3 Turbine Specifications

Rated Power	550 kW
Rotor Diameter	40 m
Rated Rotor Speed	37.1 RPM
Generator Type	Type 4 (Full power conversion)

The CART3 is a variable-speed pitch-controlled turbine that currently operates at 550 kW de-rated from 600 kW due to resonance issues.[7] The CART3 was modified for use with controls research. It is equipped with an extensive suite of sensors that is not typically available in commercial turbines. Additionally, it features a custom control system that facilitates simple inclusion of externally designed control algorithms. This research makes extensive use of this capability. In addition to this study, the CART3 is being used in other ongoing controls studies.[8]

2. BlueScout Technologies OCS LIDAR Description

NREL is collaborating with BlueScout Technologies through a Cooperative Research And Development Agreement (CRADA) to evaluate and field test BlueScout Technologies' OCS LIDAR for use in feed-forward pitch controls. Figure 2 shows the OCS LIDAR mounted to the CART3 guard-rail at the rear of the turbine's nacelle. The OCS LIDAR points toward the rotor to obtain wind speed measurements at a certain preview distance at three locations within the cone depicted in Figure 3. The OCS LIDAR is able to detect if the laser beam is blocked by one of the turbine's blades in order to prevent erroneous data being sent to the controller.

The OCS LIDAR used in these tests utilizes three fixed pulsed laser beams. It measures the Doppler shift in light received along each beam from the backscatter off of particulates in the airflow upwind of the turbine. From these multiple inputs, a resulting speed and direction of the inflow is determined for use in the feed-forward controls.

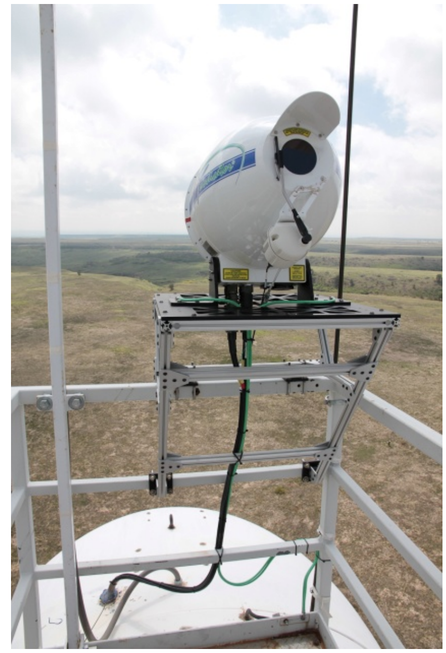

Figure 2: The BlueScout Technologies OCS LIDAR mounted on the CART3 nacelle guard-rail. (Photo credit: Lee Jay Fingersh, NREL)

3. Feed-forward Controls Overview

This section provides a brief review of the controller that is implemented and field-tested on the CART3. Figure 4 shows the role of feed-forward control (red). Most wind turbine controls consist of a feedback only component (blue), depending on measured turbine outputs. For example, in Region III, generator speed is measured and provided as the feedback signal to the pitch controller. Rotor collective pitch is commanded by the controller to regulate turbine speed to a set-point in the midst of wind speed disturbances.

To provide tight speed regulation, pitch actuation with high bandwidth is necessary.[9] However, the higher bandwidth tends to increase loading throughout the turbine.[9] Hence, with a feedback only controller, maintaining tight speed regulation is typically balanced against minimizing the loads experienced by the wind turbine. It has been proposed that with the use of a LIDAR, sufficient speed regulation can be achieved by the feed-forward controller in the low frequency ranges.[9,10] This allows for the feedback controller to be redesigned with lower gains which will result in lower pitch actuation and lower loads experienced by the turbine.[9,10] The feedback controller together with the LIDAR based feed-forward controller could then be used to command the collective pitch of the wind turbine to achieve load reduction without compromising the speed regulation. The goal of this research is to show that augmenting the standard feedback controller with a LIDAR feed-forward term will lead to further rejection of the wind disturbance in the frequency ranges where there is good coherence between LIDAR measurements and rotor wind speeds. By keeping the feedback controller unchanged, any

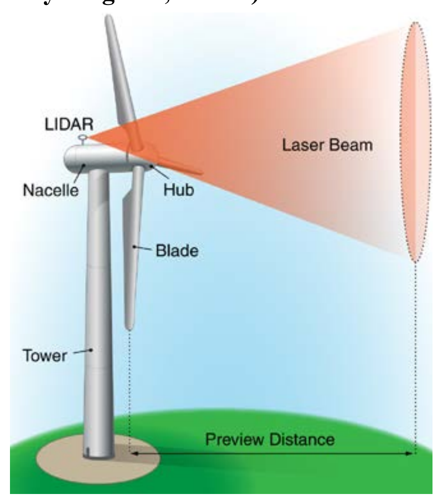

Figure 3: Typical nacelle based LIDAR measurement pattern. (Illustration by Al Hicks, NREL)

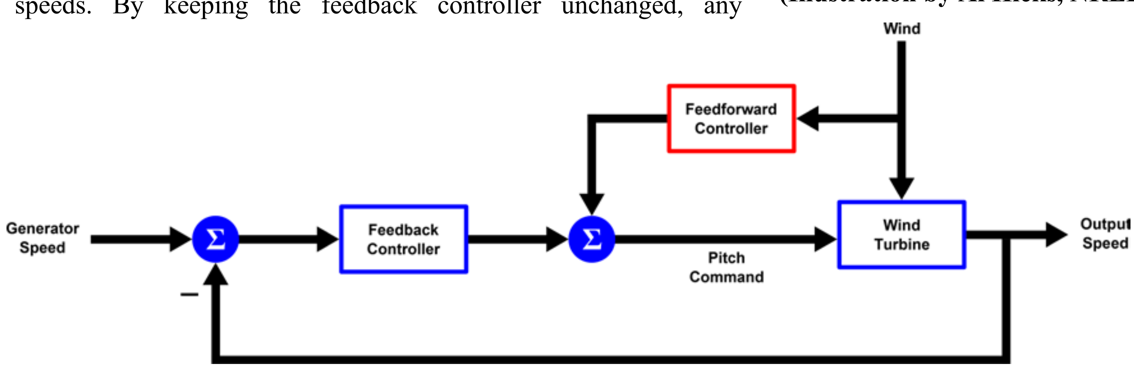

Figure 4: Feed-forward Control added to a typical feed-back controller. The wind speed signal to the feed-forward controller is obtained with a LIDAR.

improvements can be credited to the feed-forward controller.

If wind speed can be measured in front of the turbine, a feed-forward controller can assist the feedback controller in regulating turbine speed. A pitch command produced from the feed-forward controller is added to the pitch command from the feedback controller. The challenge is to provide an accurate wind speed signal to the feed-forward controller in order to improve speed regulation. LIDAR has been shown to provide such a signal.[11]

The feed-forward controller described in this paper is based on the work of David Schlipf.[12] The feed-forward pitch command is obtained from a rotor effective wind speed that is determined from the longitudinal wind speed measured by the OCS LIDAR a certain distance upwind of the rotor.

The pulsed BlueScout Technologies OCS measures the wind field along the line of sight of three independent fixed beams at three range gates upwind of the CART3 (see Figure 3). Horizontal wind speed and direction as well as vertical wind speed and angle are derived from these measurements and then transferred to the control system for each range gate. Only the first range gate at 50m is used in this work. In the control system, the longitudinal wind component is calculated from the horizontal wind speed and direction, which is then used as the LIDAR estimate of the rotor effective wind speed, v_{0L}. From the turbine data and turbine parameters a turbine estimate of the rotor effective wind speed, v_0, is calculated with an estimator based on work by van der Hooft and van Engelen[13] to evaluate the quality of the LIDAR estimate.

The internal turbine model of the estimator is modeled by:

$$J\,\dot{\Omega} + M_{LSS} = M_a(\Omega, \theta, v_0) \tag{1a}$$

$$M_a(\Omega, \theta, v_0) = \frac{1}{2}\,\rho\,\pi R^3 \frac{c_P(\lambda, \theta)}{\lambda}\, v_0^2 \tag{1b}$$

$$\lambda = \frac{\Omega R}{v_0} \tag{1c}$$

Parameters such as inertia J, rotor radius R, and the power coefficient $c_P(\lambda, \theta)$ are assumed to be known,[14] and data such as the rotor shaft torque M_{LSS}, pitch angle θ, rotor speed Ω, and air density ρ are measurable. Therefore, the only unknown is the rotor effective wind v_0. Due to the λ-dependency of the power coefficient $c_P(\lambda, \theta)$ no explicit solution can be found. Therefore, a three dimensional look-up-table $v_0(\Omega, \theta, M_a)$ is calculated a priori from the cubic equation (1b), including (1c). Here the equation (1b) is solved first in λ for numerical reasons. The aerodynamic torque $M_a(\Omega, \theta, v_0)$ can then be calculated on line from turbine data with (1a).

A comparison of all 5-minute mean values of v_0 and v_{0L} shows that the LIDAR system is able to estimate the rotor effective wind speed independent from the yaw angle of the turbine (see Figure 5). The met mast gives a good estimate only when the wind direction is aligned with the met mast directly upwind of the turbine. In addition to a time averaged analysis, the LIDAR signals also show a good correlation second by second in a time history plot (see Figure 6).

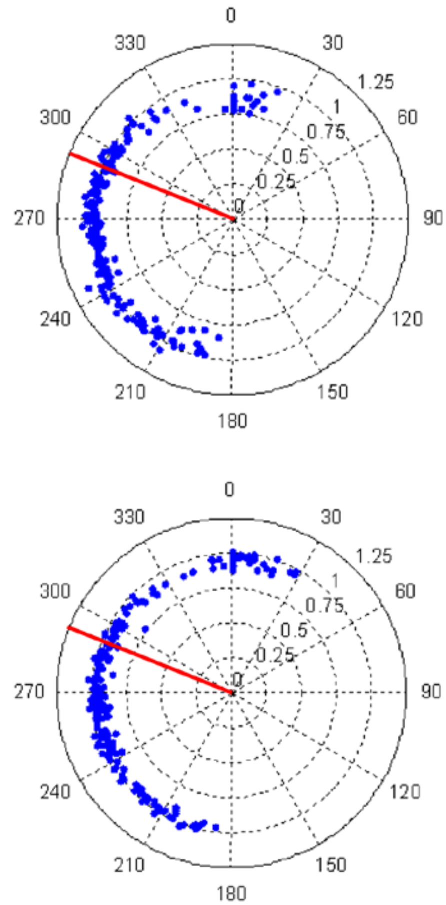

Figure 5: Distribution of the ratio (5 min average) between the met mast wind speed and the turbine rotor effective wind speed v_0 (top). Ratio between the LIDAR wind speed v_{0L} and the turbine rotor effective wind speed v_0 (bottom). Black line: met mast direction.

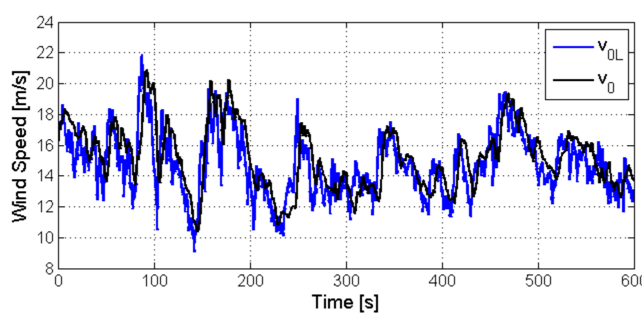

Figure 6: Rotor effective wind speed from LIDAR v_{0L} (blue) and turbine v_0 (black).

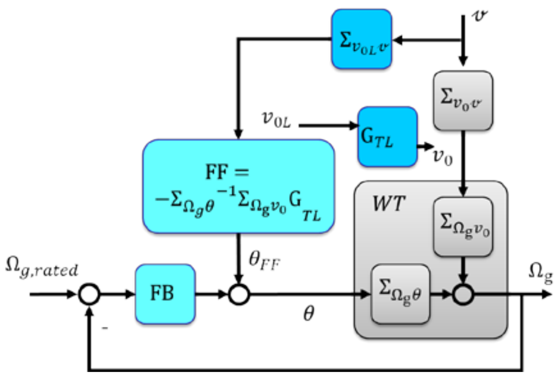

Figure 7: Control loop of LIDAR assisted feed-forward control. The LIDAR feed-forward pitch command (FF) is added to the standard feedback pitch command (FB). The resulting pitch command is fed into the wind turbine (WT).

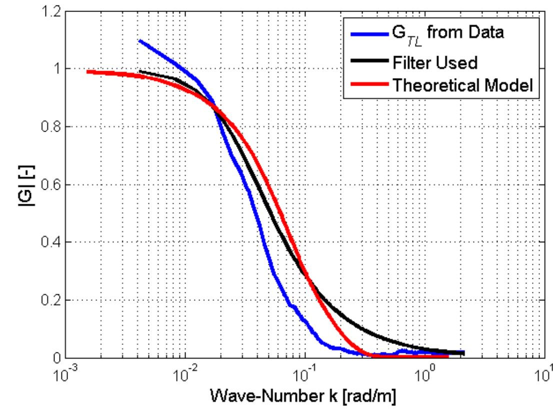

Figure 8: Transfer function G_{TL} of the rotor effective wind speed from LIDAR to turbine from data of Figure 5 (blue) and theoretical model (red) and used fitted filter (black) with a cut-off wave number at $\hat{k} = 0.03\,\frac{rad}{m}$.

Figure 7 shows that the following feed-forward controller compensates all disturbances from the wind field υ to the generator speed Ω_g:

$$\mathrm{FF} = -\Sigma^{-1}_{\Omega_g\theta}\,\Sigma_{\Omega_g v_0}\,\Sigma_{v_0\upsilon}\,\Sigma^{-1}_{v_{0L}\upsilon}, \qquad (2)$$

where $\Sigma_{\Omega_g v_0}$ and $\Sigma_{\Omega_g\theta}$ are the nonlinear subsystems transferring the wind and the pitch angle to the generator speed, $\Sigma_{v_0\upsilon}$ is the wind evolution, and $\Sigma_{v_{0L}\upsilon}$ the LIDAR measurement. The part $-\Sigma^{-1}_{\Omega_g\theta}\,\Sigma_{\Omega_g v_0}$ can be obtained by turbine modeling and a static feed-forward function is used as proposed in,[10] but wind evolution and the LIDAR measurement are difficult to model. Therefore $\Sigma_{v_0\upsilon}\,\Sigma^{-1}_{v_{0L}\upsilon}$ is approximated by a transfer function:

$$\mathrm{G}_{TL} = \frac{\mathrm{S}_{TL}}{\mathrm{S}_{LL}}, \qquad (3)$$

where S_{TL} is the cross spectrum between the LIDAR estimate and the turbine estimate and S_{LL} is the auto spectrum of the LIDAR estimate. A first order low pass filter is then fitted to the transfer function in the wave-number domain similar to the work of Schlipf et al.;[12] the maximum wave-number $\hat{k} = 0.03\,\frac{rad}{m}$ at -3dB is used for the cut-off-frequency. Turbulent eddies down to 200 m can be detected in the LIDAR and turbine data (see Figure 8). However, the theoretical maximum[15] of $0.04\,\frac{rad}{m}$ was not reached, which could have been due to the interference of the LIDAR beam with the met mast and guy wires.

4. Field Implementation and Tests

The CART3 controls software has been updated to make implementation of new control algorithms very straightforward and efficient. The entire CART3 supervisory control system is written in National Instruments LabVIEW system design software. New control algorithms can be designed in MATLAB Simulink and compiled to a dynamic-link library (DLL) to be ported into LabVIEW. The feed-forward controller was implemented in the CART3 LabVIEW system in February 2012. Field tests with this feed-forward controller receiving LIDAR wind speed signals from BlueScout Technologies' OCS LIDAR were conducted through the fall of 2012.

5. Results

The feed-forward controller described in Section 4 was field tested for a range of Region III wind speeds to show the effects of feed forward control on generator speed regulation. Several 5-minute datasets were collected with control switching between feedback only (Baseline) and feedback plus LIDAR feed-forward term (LIDAR + Baseline). The feedback controller was not modified to isolate the effect of the LIDAR term; however, future work should focus on designing the optimal feedback/feed-forward controller. Figure 9 shows that the data collected with each of these controllers covers a wide range of wind speeds and turbulence intensities. A power spectral density plot was calculated from the turbine's generator speed signal and is shown in Figure 10. This spectral plot with linear scale is based on 2430 seconds of collected data and shows that the feed-forward controller using the OCS LIDAR wind speed inputs reduces the spectral peak at low frequency. With this, the mean rotor speed standard deviation was reduced by 13.6%. The reduction in rotor speed variation shows that the feed-forward controller is able to reject the wind disturbance at low frequencies proving the concept put forth by literature. Specifically, these tests show compensation of generator speed with feed-forward control is effective with mean wind speeds in the range of $\bar{u} = 12\frac{m}{s}$ to $\bar{u} = 18\frac{m}{s}$ at low frequencies up to around $f = \frac{\hat{k}\bar{u}}{2\pi} = 0.1$ Hz.

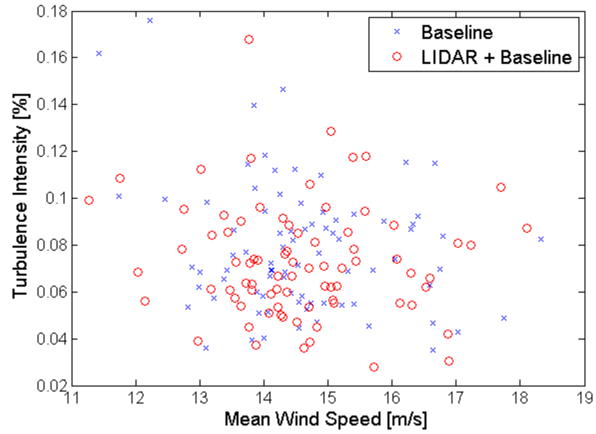

Figure 9: Distribution of the wind measurement data collected over a wide range of wind speeds and turbulence intensities.

In addition to the spectra of the generator speed, the power spectral densities of the tower fore-aft bending moment, measured rotor torque, and the collective blade flap bending moment were also investigated. Figure 11 shows the spectra of the tower fore-aft bending moment. Due to the CART3's high aerodynamic damping, the fore-aft bending is not dominated by any resonant mode. However, reductions can be seen at lower frequencies when the LIDAR feed-forward term is included with the feedback controller similar to the results of the generator speed spectra.

Figure 12 shows the spectra of the rotor shaft torque. The peak at 2.7 Hz is the first drivetrain mode, 2 Hz is from the first collective flap bending mode, and 0.6 Hz is from the 1P forcing mode. All of these modes are above the threshold where reductions were expected. With the inclusion of the LIDAR feed-forward term, no significant increases were found, and there were slight reductions. Figure 13 shows the spectra of the collective flap bending moment. A slight reduction can be found at low frequencies similar to the generator speed, and tower fore-aft bending moment. Reductions are also found at 2 Hz (collective blade flap mode), similar to the results found with the rotor shaft torque. Again, no significant increases were found by including the LIDAR feed-forward term.

Damage equivalent loads were also computed from the data collected to see if including the LIDAR feed-forward term had any adverse effects on the wind turbine. An S/N slope of m=4 (corresponding to steel) was used for the tower bending moments and rotor torque. Additionally, an S/N slope of m=10 (corresponding to fiberglass) was used for the blade bending moments. Table 2 shows the damage equivalent loads that were calculated for both

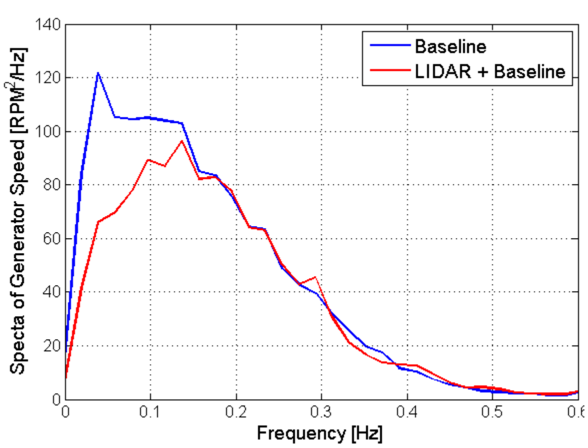

Figure 10: Spectra of the generator speed, showing wind disturbance compensation for low frequencies with the LIDAR feed-forward term. This shows that LIDAR measurements can be used to further reject the wind disturbance.

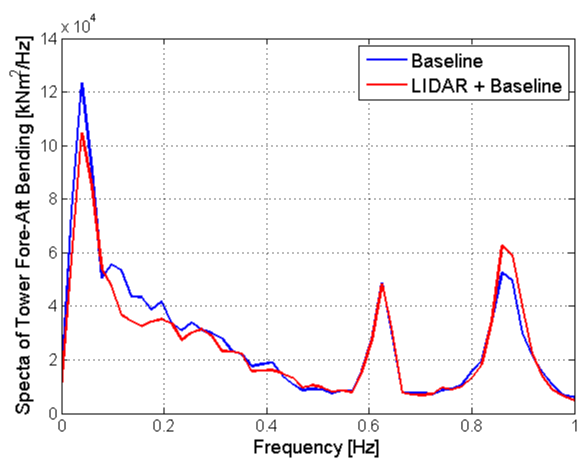

Figure 11: Spectra of the tower fore-aft bending. No resonant mode dominates due to the CART3's high aerodynamic damping. Reductions are still seen at lower frequencies with the LIDAR feed-forward term.

cases. Only minor reductions in the loads were expected, because the goal of this work was to see the effects of using a LIDAR for feed-forward controls without optimizing the feedback controller for load mitigation. The results from Table 2 show that by using the LIDAR feed-forward term the flap bending and rotor torque are substantially reduced compared to the small increases in the side-side bending and blade edge bending. Similar to the spectra results for the tower fore-aft bending, a reduction was found in the damage equivalent load as well. Additionally, because the tower side-side bending moment and blade edge bending moments are not coupled to the collective pitch control, the loads will most likely average out to no difference with a large enough data set for both cases.

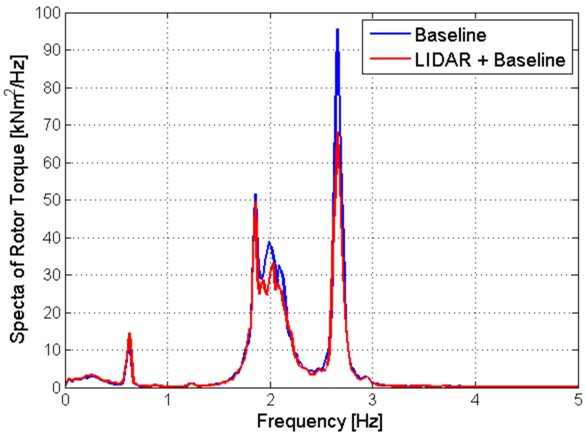

Figure 12: Spectra of the rotor torque. The dominant resonant modes are above the threshold of the LIDAR's capabilities. Reductions are still found with the LIDAR feed-forward term.

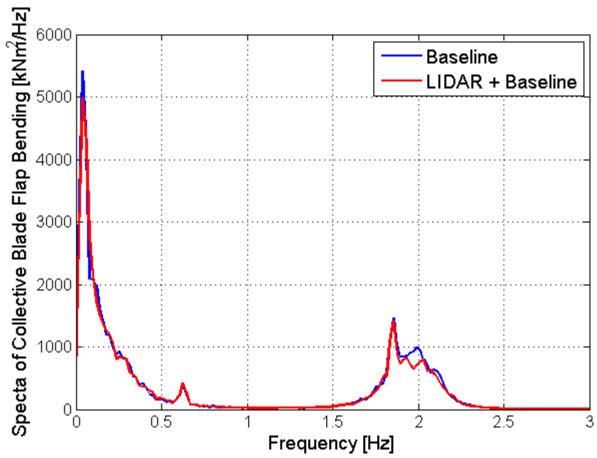

Figure 13: Spectra of the collective blade flap bending. Slight reductions are seen with the use of the LIDAR feed-forward term.

Table 2: Damage Equivalent Loads Comparison

Load:	Baseline:	LIDAR + Baseline:	Change from Baseline:
Tower Fore-Aft Bending	503.4 kN-m	494.6 kN-m	-1.8%
Tower Side-Side Bending	475.8 kN-m	488.2 kN-m	2.6%
Blade 1 Flap Bending	273.7 kN-m	253.8 kN-m	-7.3%
Blade 1 Edge Bending	304.1 kN-m	304.7 kN-m	0.20%
Rotor Torque	22.79 kN-m	20.55 kN-m	-9.8%

6. Summary and Conclusion

This work shows that a fixed-beam pulsed LIDAR can obtain preview information about the incoming wind field. The LIDAR showed good correlation to the turbine's rotor effective wind speed independent of the turbine's yaw angle unlike the met mast's correlation which needed the wind direction to be aligned between the met mast and the turbine. The LIDAR's estimate of the rotor effective wind speed was then filtered so that it could be fed into the controller before the wind disturbance affected the turbine. Using this feed-forward control strategy, the controller provided a corrected pitch command to the feedback only controller. This controller was then field tested to determine if the feed-forward controller would be able to reject the wind disturbance at low frequencies. Comparing results from a broad range of wind conditions confirmed that the feed-forward controller rejected the wind disturbance by reducing the generator speed variation at low frequencies up to around 0.1 Hz, which is consistent with the frequency of the detected correlation. Additionally, a spectral analysis of the turbine loads showed some reductions for the tower fore-aft bending, rotor torque, and collective flap bending. A damage equivalent loads analysis also showed reductions in these three loads, and slight increases in the tower side-side and blade edge bending loads. However, because the tower side-side and blade edge bending loads are not coupled to the collective pitch control, a larger data set should show the feedback and feedback plus feed-forward loads averaging out to the same value.

This study shows that LIDAR can be used for feed-forward control and it confirms the predictions in the literature. Future work should look into optimizing the feedback controller to take further advantage of the benefits of LIDAR-based disturbance rejection. For example, the PI gains of the feedback controller can be reduced such that the speed regulation with the LIDAR is still adequate, but the lower feedback gains will provide reductions in loading relative to the baseline case. Furthermore, as the technology of LIDAR systems matures, improved correlation between the LIDAR estimate and the actual wind speed can be achieved, which could be used to provide further rejection of the wind disturbance. These technological advances would provide better speed regulation from the feed-forward controller allowing for further load reductions to be achieved by the feedback controller.

Acknowledgments

The authors wish to offer special thanks to Andrew Hopkins and Al Iaconangelo along with others at BlueScout Technologies for providing the technical support for the OCS LIDAR. The authors wish to also thank all of the technicians at the NWTC for their support in maintaining and operating the CART 3 wind turbine.

NREL's contributions to this report were funded by the Wind and Water Power Program, Office of Energy Efficiency and Renewable Energy of the U.S. Department of Energy under contract No. DE-AC02-05CH11231. The authors are solely responsible for any omission or errors contained herein.

References

[1]Wright, A.D., and Balas, M.J., "Design of State-Space-Based Control Algorithms for Wind Turbine Speed Regulation," *ASME Journal of Solar Energy Engineering*, vol. 125, no. 4, November 2003, pp. 386–395.

[2]Wright, A.D., and Balas, M.J., "Design of Controls to Attenuate Loads in the Controls Advanced Research Turbine," *ASME Journal of Solar Energy Engineering*, vol. 126, no. 4, November 2004, pp. 1083–1091.

[3]Wright, A. D., *Modern Control Design for Flexible Wind Turbines*, NREL Report TP-500-35816, Golden, CO: National Renewable Energy Laboratory, 2004.

[4]Stol, K.A., and Balas, M.J. "Periodic Disturbance Accommodating Control for Blade Load Mitigation in Wind Turbines," *ASME Journal of Solar Energy Engineering*, vol. 125, no. 4, November 2003, pp. 379–385.

[5]Wright, A.D., Stol, K.A., and Fingersh, L.J. "Progress in Implementing and Testing State-Space Controls for the Controls Advanced Research Turbine," 24th ASME Wind Energy Conference, Reno, Nevada, 2005, pp. 88–100.

[6]Dunne, F., Simley, E., and Pao, L. Y. *LIDAR Wind Speed Measurement Analysis and Feed-Forward Blade Pitch Control for Load Mitigation in Wind Turbines*, NREL/SR-5000-52098, Golden, DO: National Renewable Energy Laboratory, 2011.

[7]Fleming, P. A., Wright, A.D., Fingersh, L.J., and van Wingerden, J.W. "Resonant Vibrations Resulting from the Re-Engineering of a Constant-Speed 2-Bladed Turbine to a Variable-Speed 3-Bladed Turbine, " *49th AIAA Aerospace Sciences Meeting*, 2011, Orlando Florida.

[8]Fleming, P.A., van Wingerden, J.W., and Wright, A.D. "Comparing State-Space Multivariable Controls to Multi-SISO Controls for Load Reduction of Drivetrain-Coupled Modes on Wind Turbines through Field-Testing," *50th AIAA Aerospace Sciences Meeting*, 2012, Nashville, Tennessee.

[9]E. A. Bossanyi, Kumar, A. and Hugues-Salas, O., "Wind Turbine Control Applications of Turbine-Mounted LIDAR," *Proc. Science of Making Torque*, 2012, in press.

[10]Schlipf, D., Fischer, T., Carcangiu, C. E., Rossetti, M., and Bossanyi, E., *Load Analysis of Look-Ahead Collective Pitch Control Using LIDAR*, DEWEK, Bremen, Germany, November 2010.

[11]Schlipf, D. Trabucchi, O., Bischoff, M., Hofsäß, J., Mann, T., Mikkelsen, A., Rettenmeier, J.J., Trujillo and Kühn, M., "Testing of Frozen Turbulence Hypothesis for Wind Turbine Applications with a Scanning LIDAR System, ISARS Conference, 2010.

[12]Schlipf, D. Fleming, P. Haizmann, F. Scholbrock, A. Hofsäß, M. Wright, A. Cheng, P.W., "Field Testing of Feedforward Collective Pitch Control on the CART2 Using a Nacelle-Based Lidar Scanner" *Proc. Science of Making Torque*, 2012, in press.

[13]van der Hooft, E.L., and van Engelen, T. G., "Estimated Wind Speed Feed-Forward Control for Wind Turbine Operation Optimization, EWEC, London, UK, Novermber 2004.

[14]Stol, K., *Geometry and Structural Properties for the Controls Advanced Research Turbine (CART) from Model Tuning*, NREL/SR-500-32087,.National Renewable Energy Laboratory, Golden, CO , 2004.

[15]Schlipf, D., Mann, J., Rettenmeier, A., and Cheng, P.W. *Model of the Correlation between Lidar Systems and Wind Turbines for Lidar Assisted Control*, ISARS Conference, 2012.